SMOOTH SAMPLING TRAJECTORIES FOR SPARSE RECOVERY IN MRI

Rebecca M. Willett

Department of Electrical and Computer Engineering
Duke University, Durham, NC 27708

ABSTRACT

Recent attempts to apply compressed sensing to MRI have resulted in pseudo-random k-space sampling trajectories which, if applied naïvely, may do little to decrease data acquisition time. This paper shows how an important indicator of CS performance guarantees, the Restricted Isometry Property, holds for *deterministic* sampling trajectories corresponding to radial and spiral sampling patterns in common use. These theoretical results support several empirical studies in the literature on compressed sensing in MRI. A combination of Geršgorin's Disc Theory and Weyl's sums lead to performance bounds on sparse recovery algorithms applied to MRI data collected along short and smooth sampling trajectories.

***Index Terms*—** compressed sensing, MRI trajectory, exponential sums, restricted isometry property

1 MR Sampling and Compressed Sensing

Inspired by the seminal work on compressed sensing (CS) presented in [1], the magnetic resonance (MR) community has been carefully investigating how CS ideas might help improve the quality of MR images while reducing data acquisition time [2]. However, much of the existing CS theory is predicated on pseudo-random sampling patterns which, if implemented naïvely in modern MR imagers, yield longer sampling trajectories than the radial and spiral patterns commonly used. Several investigators have studied random undersampling patterns along radial and spiral sampling trajectories [3, 4, 5, 6, 7], producing very promising empirical results.

Nevertheless, there is a pervasive disconnect between the random sampling patterns proposed in the CS community and the smooth and fast sampling trajectories favored by the MR community. This discord stems from the different motivations underlying CS and MR sampling techniques: while CS aims to limit the *number* of samples collected, MR data acquisition time depends on the *length and curvature of the sampling path*. In this paper, we present new theoretical findings on *deterministic* sampling trajectories for MR which closely approximate radial and spiral sampling patterns yet satisfy key properties (i.e., the Restricted Isometry Property) associated with CS.

This contribution sheds new light on one of the early and famous experiments in CS. In [1], Candès et al showed that a Shepp-Logan phantom could be reconstructed perfectly from k-space samples collected in a radial pattern common to modern MRI scanners. The accompanying theory, however, did not directly justify that sampling strategy. Rather, the authors assumed that samples were collected at *random* locations in the Fourier domain. This paper shows that (near) radial or spiral sampling in k-space of sparse or sparse-gradient images is also sufficient for accurate reconstruction, while offering the additional advantage of corresponding to short and smooth sampling trajectories and associated short scan times.

This is an invited paper in the special session on "Compressive sensing for biomedical imaging." The work is supported by NSF Career Award No. CCF-06-43947, NSF Grant No. DMS-08-11062, and AFRL Grant No. FA8650-07-D-1221.

2 Problem formulation

Let f denote the MR image of interest, and assume f is either (a) sparse in the spatial domain or (b) has a sparse gradient. In particular, in case (a) we have

$$f(x) = \sum_{z \in \mathsf{Z}} \alpha_z \delta(x - z)$$

for $x \equiv (x_1, x_2) \in [0,1)^2$, where

$$\mathsf{Z} \triangleq \left\{0, \frac{1}{M}, \frac{2}{M}, \ldots, \frac{M-1}{M}\right\}^2$$

is a set of 2d spatial locations and $\{\alpha_z : z \in \mathsf{Z}\}$ is a set of real-valued amplitudes. We assume that all but $K \ll M^2$ of the α_zs are zero-valued.

Samples are collected sequentially in the Fourier domain (i.e. "k-space"). The n^{th} sample is collected at frequency $\omega_n \equiv (\omega_{n,1}, \omega_{n,2}) \in (-1,1)^2$ [need to handle this in theory...]. We model k-space sampling along a trajectory as

$$\begin{aligned} y_n &= \frac{1}{\sqrt{N}} \int_{[0,1)^2} f(x) e^{-i2\pi\langle x, \omega_n \rangle} dx \\ &= \sum_{z \in \mathsf{Z}} \frac{\alpha_z}{\sqrt{N}} \int_{[0,1)^2} \delta(x - z) e^{-i2\pi\langle x, \omega_n \rangle} dx \\ &= \sum_{z \in \mathsf{Z}} \frac{\alpha_z}{\sqrt{N}} e^{-i2\pi\langle z, \omega_n \rangle}. \end{aligned}$$

Set

$$\phi_{z,\omega} \triangleq \frac{1}{\sqrt{N}} e^{i2\pi\langle z,\omega\rangle}$$

and let

$$\Phi \triangleq [\phi_{z,\omega}]^T_{\substack{z\in \mathsf{Z} \\ \omega\in\{\omega_1,\ldots,\omega_N\}}}$$

be an $N \times M^2$ matrix. Let α denote the length-M^2 vector whose elements are members of the set $\{\alpha_z : z \in \mathsf{Z}\}$ and $y \triangleq [y_1, \ldots, y_N]^T$. We then have

$$y_n = \sum_{z\in\mathsf{Z}} \alpha_z \phi_{z,\omega_n} \tag{1a}$$

$$y = \Phi\alpha. \tag{1b}$$

Alternatively, in case (b) where the image gradient is assumed sparse, we have

$$\begin{aligned} D_v f(x) &= \sum_{z\in\mathsf{Z}} \alpha_z \delta(x - z) \\ D_h f(x) &= \sum_{z\in\mathsf{Z}} \beta_z \delta(x - z) \end{aligned} \tag{2}$$

where

$$D_v f(x) = f(x_1, x_2) - f(x_1 - 1/M, x_2) \qquad \text{and}$$
$$D_h f(x) = f(x_1, x_2) - f(x_1, x_2 - 1/M)$$

correspond to vertical and horizontal discrete gradients. As before, we assume that all but $K \ll M^2$ of the α_z's and β_z's are zero-valued.

In this case, our k-space samples are the same as above, and (as suggested in [8]) we multiply each sample by a complex exponential to account for the gradient as follows:

$$\begin{aligned} y_n^v &\triangleq y_n \left(1 - e^{-i2\pi\omega_{n,1}/M}\right) \\ &= \frac{1}{\sqrt{N}} \int_{[0,1)^2} f(x) \left(1 - e^{-i2\pi\omega_{n,1}/M}\right) e^{-i2\pi\langle x,\omega_n\rangle} dx \\ &= \frac{1}{\sqrt{N}} \int_{[0,1)^2} D_v f(x) e^{-i2\pi\langle x,\omega_n\rangle} dx \\ &= \sum_{z\in\mathsf{Z}} \frac{\alpha_z}{\sqrt{N}} \int_{[0,1)^2} \delta(x - z) e^{-i2\pi\langle x,\omega_n\rangle} dx \\ &= \sum_{z\in\mathsf{Z}} \frac{\alpha_z}{\sqrt{N}} e^{-i2\pi\langle z,\omega_n\rangle} \end{aligned}$$

with y_n^h defined similarly. Let α denote the length-$(2M^2)$ vector whose elements are members of the sets $\{\alpha_z : z \in \mathsf{Z}\}$ and $\{\beta_z : z \in \mathsf{Z}\}$, and let $y \triangleq [y_1^v, \ldots, y_N^v, y_1^h, \ldots, y_N^h]^T$. Then, as before,

$$y = \Phi\alpha.$$

Our goal is to choose a sampling path $\omega(t)$ and associated sample locations $\omega_n \triangleq \omega(n/N)$ such that the resulting sensing matrix Φ satisfies the Restricted Isometry Property (RIP), meaning sparse recovery methods can be successfully applied to estimating α (and hence f) in either noisy or noisy-free settings. These concepts are reviewed below.

3 CS Performance Guarantees

Much of the CS literature revolves around determining when a sensing matrix Φ allows accurate reconstruction using an appropriate algorithm. One widely used property used in such discussions is the Restricted Isometry Property (RIP), proposed in [9]:

Definition 1 *(Restricted Isometry Property). The matrix Φ satisfies the Restricted Isometry Property of order K with parameter $\delta_K \in [0, 1)$ if*

$$(1 - \delta_K)\|\alpha\|_2^2 \le \|\Phi\alpha\|_2^2 \le (1 + \delta_K)\|\alpha\|_2^2$$

holds simultaneously for all sparse vectors α having no more than K nonzero entries. Matrices with this property are denoted RIP(K, δ_K).

Matrices which satisfy the RIP combined with sparse recovery algorithms are guaranteed to yield accurate estimates of the underlying function f:

Theorem 1 (Sparse Recovery with RIP [9, 10, 11].) *Let Φ be a matrix satisfying RIP$(2K, \delta_{2K})$ with $\delta_{2K} < \sqrt{2} - 1$, and let $y = \Phi\alpha$ be a vector of observations of any sparse signal $\alpha \in \mathbb{R}^{M^2}$ having no more than K nonzero entries. Then the estimate*

$$\widehat{\alpha} = \arg\min_a \|a\|_1 \qquad \textit{subject to} \qquad y = \Phi a$$

is unique and equal to α.

Similar results have been derived for noise-corrupted measurements (cf. [12]).

4 Main result

The central thesis of this paper is based upon the theoretical foundation established in [13], which showed the following:

Theorem 2 (CS Sampling Trajectories [13].) *Let $d \ge 4$. Then the path $\omega(t) = (t^{d-1}, t^d)$ and associated sample points $\omega_n = \omega(n/N)$, $n = 1, \ldots, N$ satisfies RIP(K,δ_K) for $\delta_K < \sqrt{2} - 1$ and*

$$K \le \delta_K e^{-3d} N^{\frac{1}{24d^2 \log d}}.$$

This theorem is proved in [13] using a combination of Geršgorin's Disc Theorem [14, 15] and Weyl's sums [16].

Remark 1 *The trajectory described in Theorem 2 satisfies the RIP, and so is guaranteed to yield accurate estimates of f via an appropriate sparse reconstruction method. Note that for larger d, the corresponding trajectory is closer to being a straight line and hence has a shorter pathlength; however, for a fixed N larger d also implies a smaller upper bound on K, the maximum number of nonzero elements in α we may tolerate.*

Remark 2 *When f is real-valued, it's Fourier transform (denoted $F(\omega)$) is circularly symmetric; i.e., if $F(\omega) = F^*(-\omega)$. In this case, we may double the trajectory to traverse the entire k-space by setting*

$$\omega_n = \begin{cases} -\omega(n/N), & \text{if} \quad 1 \leq n \leq N \\ \omega((n-N)/N), & \text{if} \quad N < n \leq 2N; \end{cases}$$

the resulting trajectory, displayed in Figure 1(b), also satisfies the RIP.

Remark 3 *On a practical note, when the original image is not highly sparse, it may be difficult to satisfy Theorem 2 because sampling locations are naturally quantized by the MRI hardware. In this case, accurate sparse recovery can be guaranteed by taking the sampling trajectory in Theorem 2 and repeating it at evenly-spaced rotations around the center of k-space; the resulting asterisk-like pattern would closely match conventional radial sampling trajectories in MRI.*

Corollary 1 (Spiral trajectories) . *Consider the spiral trajectory*

$$\widetilde{\omega}(t) = \begin{pmatrix} at\cos(bt) \\ at\sin(bt) \end{pmatrix} \tag{3}$$

for two constants $a, b > 0$. Let $\omega(t)$ be the order-$(2b)$ Taylor series approximation to this trajectory; i.e., choose

$$\omega(t) = \begin{pmatrix} at - \frac{ab^2t^3}{2!} + \frac{ab^4t^5}{4!} - \cdots \\ \\ abt^2 - \frac{ab^3t^4}{3!} + \frac{ab^5t^6}{5!} - \cdots \end{pmatrix} \tag{4}$$

and associated sample points $\omega_n = \omega(n/N)$, $n = 1, \ldots, N$. Then the resulting sensing matrix Φ satisfies RIP(K,δ_K) for $\delta_K < \sqrt{2} - 1$ and

$$K \leq \delta_K e^{-6b} N^{\frac{1}{96b^2 \log 2b}}.$$

Remark 4 *The spiral trajectory described in Corollary 1 combined with the sparse gradient assumption formalized in* (2) *lend strong theoretic support to the empirical studies conducted in [3, 4], in which undersampling was conducted along spiral trajectories and total variation regularization during the reconstruction exploited sparse gradients.*

5 Examples

The images in Figure 1 depict the above principles applied to a phantom MRI image which comes standard with MATLAB and has a sparse gradient as in (2). In particular, Figure 1(a) is the original phantom image, and Figures 1(b-d) display the magnitude of the Fourier transform of this phantom beneath various sampling trajectories supported by the above theory. The trajectory in Figure 1(b) is computed using a polynomial of degree $d = 4$ (the minimum allowed according to Theorem 2), while the trajectory in Figure 1(c) is computed using a polynomial of degree $d = 20$. Note that the $d = 20$ trajectory more closely approximates the radial trajectory commonly used in practice, but the sampling locations are more nonuniformly spaced along this path relative to the spacing for $d = 4$. In both these cases, the length of the trajectory is $O(1)$, much less than the $O(\sqrt{N})$ trajectory length which would correspond to N randomly distributed sampling locations.

The green path in Figure 1(d) corresponds to a spiral trajectory as in (3) for $a = 1$ and $b = 20$; the red dots along this path correspond to sample locations computed using the Taylor series approximation to the spiral in (4) in Corollary 1. The length of this spiral [17] is

$$\frac{a}{2b}\left[b\sqrt{1+b^2} + \log_e(b + \sqrt{(}1+b^2))\right],$$

which is $O(1)$ with respect to the sparsity level K, number of sampling points N, and spatial resolution M.

6 Conclusions

This paper provides theoretical justification for common MRI sampling trajectories, radial and spiral, from a compressed sensing perspective. In particular, we demonstrates that for a given deterministic set of sampling locations along spiral and radial trajectories, the resulting projection matrix satisfies the Restricted Isometry Property and hence leads to accurate high-resolution MR imagery if appropriate sparsity-promoting or total-variation reconstruction algorithms are used.

7 References

[1] E. J. Candès, J. Romberg, and T. Tao, "Robust uncertainty principles: Exact signal reconstruction from highly incomplete frequency information," *IEEE Trans. Info. Th.*, vol. 52, pp. 489–509, 2004.

[2] M. Lustig, D. Donoho, and J. M. Pauly, "Sparse mri: The application of compressed sensing for rapid mr imaging," *Magnetic Resonance in Medicine*, vol. 58, no. 6, pp. 1182–1195, 2007.

[3] M. Lustig, J. H. Lee, D. L. Donoho, and J. M. Pauly, "Faster imaging with randomly perturbed, undersampled spirals and ℓ_1 reconstruction," in *Proceedings of the 13th Annual Meeting of ISMRM*, 2005.

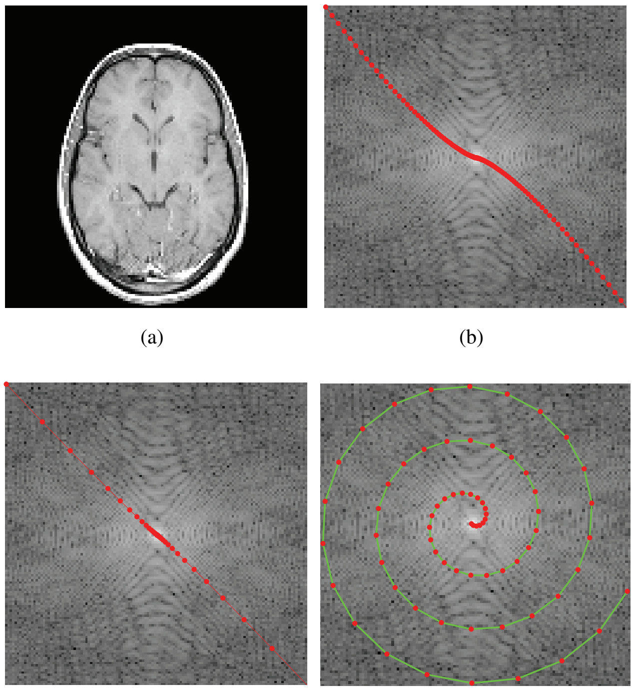

(a) (b)

(c) (d)

Fig. 1. Sample trajectories and sampling locations in MRI which provably satisfy the Restricted Isometry Property. (a) Phantom MRI image which has a sparse gradient. (b) Sampling trajectory from Theorem 2 with $d = 4$ superimposed on the magnitude of the Fourier transform of the image in (a). (c) Sampling trajectory from Theorem 2 with $d = 20$ superimposed on the magnitude of the Fourier transform of the image in (a). Note the nonuniform spacing between sample locations and the closeness of this trajectory with the conventional radial sampling patterns common in MRI. (d) Sampling trajectory from Corollary 1 with $a = 1$ and $b = 20$ superimposed on the magnitude of the Fourier transform of the image in (a). The green line is the spiral in (3) and the red dots are the sample locations in (4).

[4] J. M. Santos, C. H. Cunningham, M. Lustig, B. A. Hargreaves, B. S. Hu, D. G. Nishimura, and J. M. Pauly, "Single breath-hold whole-heart mra using variable-density spirals at 3t," *Magn. Reson. Med.*, vol. 55, pp. 371–379, 2006.

[5] T. C. Chang, L. He, and T. Fang, "Mr image reconstruction from sparse radial samples using Bregman iteration," in *Proceedings of the 13th Annual Meeting of ISMRM*, 2006.

[6] J. C. Ye, S. Tak, Y. Han, and H. W. Park, "Projection reconstruction mr imaging using focuss," *Magn. Reson. Med.*, vol. 57, pp. 764–775, 2007.

[7] K. T. Block, M. Uecker, and J. Frahm, "Undersampled radial mri with multiple coils. iterative image reconstruction using a total variation constraint," *Magn. Reson. Med.*, vol. 57, pp. 1086–1098, 2007.

[8] R. Maleh, A. C. Gilbert, and M. J. Strauss, "Sparse gradient image reconstruction done faster," in *Proc. ICIP*, 2007.

[9] E. J. Candès and T. Tao, "Decoding by linear programming," *IEEE Trans. Inform. Theory*, vol. 15, no. 12, pp. 4203–4215, 2005.

[10] E. Candès, "The restricted isometry property and its implications for compressed sensing," *C. R. Acad. Sci., Ser. I*, vol. 346, pp. 589–592, 2008.

[11] W. U. Bajwa, *New Information Processing Theory and Methods for Exploiting Sparity in Wireless Systems*, Ph.D. thesis, University of Wisconsin–Madison, 2009.

[12] J. Haupt and R. Nowak, "Signal reconstruction from noisy random projections," *IEEE Trans. on Information Theory*, vol. 52, no. 9, pp. 4036–4048, 2006.

[13] R. Willett, "Short and smooth sampling trajectories for compressed sensing," in *IEEE International Conference on Acoustics, Speech and Signal Processing – ICASSP'11*, 2011.

[14] R. Varga, *Geršgorin and His Circles*, Springer-Verlag, Berlin, Germany, 2004.

[15] J. Haupt, L. Applebaum, and R. Nowak, "On the restricted isometry of deterministically subsampled fourier matrices," in *Proc. 44th Annual Conf. on Information Sciences and Systems (CISS)*, 2010.

[16] N. M. Korobov, *Exponential Sums and their Applications*, Kluwer Academic Press, Dordrecht, The Netherlands, 1992, Translated by Yu. N. Shakhov.

[17] E. W. Weisstein, "Archimedes' spiral," in *MathWorld–A Wolfram Web Resource*. 2011, http://mathworld.wolfram.com/ArchimedesSpiral.html.